Process optimization by response surface methodology of plasma-catalytic formaldehyde removal using MnO_x–Fe_2O_3 catalysts

Tian Chang[1,2], Zhenxing Shen[1], Savita K.P. Veerapandian[2], Rino Morent[2]

[1] *Department of Environmental Sciences and Engineering, Xi'an Jiaotong University, Xi'an 710049, China*
[2] *Research Unit Plasma Technology, Department of Applied Physics, Faculty of Engineering and Architecture, Ghent University, Sint-Pietersnieuwstraat 41 – B4, 9000 Ghent, Belgium*

Abstract: In this work, a non-thermal plasma (NTP) reactor combined with a MnO_x–Fe_2O_3 catalyst has been developed for formaldehyde removal from dry air. Catalyst characterization was performed to understand the influence of catalyst properties on the catalytic activity in the NTP-catalytic reaction process. The effects of various experimental parameters such as discharge power, gas flow rate and molar ratio of Fe/Mn and their interactions on the performance of formaldehyde degradation were evaluated using a central composite design.

Keywords: plasma, catalyst, formaldehyde.

1. Introduction

Formaldehyde (HCHO) is a toxic volatile organic compound (VOs), mainly originating from industrial processes such as the production of resins, adhesives, and cosmetics [1,2]. The emission of formaldehyde escalates the public concern due to its carcinogenic and teratogenic effects when exposed to high dose [3-5]. Conventional technologies such as adsorption, photocatalytic oxidation and catalytic oxidation have been investigated to reduce the formaldehyde concentration in air, but were limited by their low efficiency for removal of low concentrations of formaldehyde [6, 7]. In recent years, the combination of non-thermal plasma (NTP) technology and catalysts appeared to be an alternative approach for VOC degradation.

In this work, we report the systematic investigation of formaldehyde removal in the NTP-catalytic system over MnO_x-Fe_2O_3/HZSM-5 catalysts using a dielectric barrier discharge (DBD) reactor. The effect of different parameters such as discharge power, gas flow rate and molar ratio of Fe/Mn on the performance of the NTP-catalytic process for formaldehyde removal was investigated. The response surface methodology (RSM) based on the central composite design (CCD) was applied to investigate the relationship between the key process parameters and to optimize the hybrid process in terms of the formaldehyde removal efficiency and CO_2 yield. In addition, the as prepared catalysts were characterized by XRD to gain some insight about the relationship between the catalyst properties and catalytic activity in the NTP-catalytic system.

2. Experimental

2.1. Catalyst preparation and characterization

The MnO_x-Fe_2O_3 catalysts were prepared via a co-precipitation method using $Mn(NO_3)_2{\cdot}4H_2O$ and $Fe(NO_3)_3{\cdot}9H_2O$ as the precursor. During the synthesis, the appropriate amount of $Mn(NO_3)_2{\cdot}4H_2O$ and $Fe(NO_3)_3{\cdot}9H_2O$ were dissolved in deionized water by magnetic stirring. Then, appropriate amount of $KMnO_4$ (0.4 mol·L^{-1}) was added to the above solution under stirring. Then, the mixture was placed in a water bath at 60 ºC, and then the ammonium hydroxide was gradually added to the mixture until the pH reached 9, stirring continuously for 4 h. Subsequently, the products were collected by centrifugation and rinsed several times with deionized water, followed by drying and calcination.

2.2. Catalyst characterization

Phase identification of the catalysts was done by X-ray diffraction (XRD, Malvern Panalytical, the Netherlands) equipped with Cu-Kα radiation source (λ = 1.5406 Å).

2.3. Experimental setup

The schematic diagram of the experimental system is shown in Fig. 1 and it consists of a gas feeding system, the NTP-catalytic system, and a gas analysis system. The flow rate of air (N_2:O_2=4:1) and formaldehyde were controlled by a mass flow controller (MFC, Sevenstar D07-series, China) to obtain a fixed initial concentration of formaldehyde (60 ppm). The total gas flow rate was varied from 0.5 L·min^{-1} to 1.5 L·min^{-1}. An alternating-current high-voltage power supply (CTP-2000 K, Nanjing Suman Electronic Co., China) was used to power the DBD reactor. The electric signals were detected by an oscilloscope (Tektronix MDO 3012, America) and the discharge power injected into the plasma is sampled using the Manley method (V–Q Lissajous method). The gas samples were analyzed online by an FT-IR gas analyzer (Gasmet Dx 4500, Finland) with a resolution of 8cm^{-1} and gas chromatography (GC 9790 II, Fuli, China). Each experiment was repeated at least three times.

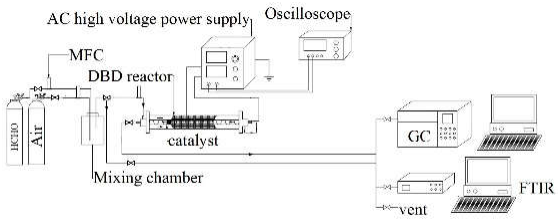

Fig. 1 Experimental setup

2.4. Modelling

A three-factor and five-level CCD was employed to investigate the effects of each process variable and the

interactions of the variables on the removal of formaldehyde in the NTP-catalytic system over MnO_x-Fe_2O_3 catalysts. In this work, the discharge power (X_1), gas flow rate (X_2), and molar ratio of Fe/Mn (X_3) were selected as the input factors, and the removal efficiency (Y_1) was employed as the responses. In the CCD design, the correlation of the independent variables and the responses can be described by a quadratic polynomial response equation as shown in Eq. (1).

$$Y = \beta_0 + \sum_{i=1}^{k} \beta_i X_i + \sum_{i=1}^{k} \beta_{ii} X_i^2 + \sum_{i=1}^{k-1} \sum_{j=2}^{k} \beta_{ij} X_i X_j + \varepsilon \quad (1)$$

where Y, k and ε are donated as the predicted response, the number of variables, and the residual value, respectively. X_i and X_j are coded as independent variables. β_0, β_i, β_{ii} and β_{iji} are donated as constant, linear, quadratic and interaction coefficients, respectively. The adequacy and fit of the models, the experimental data and plotting response surface plots were analyzed by the statistical software package Design-Expert 11 (Stat-Ease Inc., Minneapolis, USA).

3. Result and discussion

3.1. Catalyst characterization

XRD was conducted to investigate the structure of the as-prepared catalysts. Fig. 2 shows the XRD patterns of the MnO_2, Fe_2O_3 and MnO_x–Fe_2O_3 catalysts. For MnO_x catalyst, the main peaks at 12.7°, 18.0°, 28.7°, 37.5°, 38.3°, 40.9°, 41.9° and 60.0° could be primarily attributed to α-MnO_2 (JCPDS 44-141), while the diffraction signals at 33.0°, 38.3°, 45.2°, 49.5°, 55.2°, 64.2°, 65.9° and 69.3° could be indexed to Mn_2O_3 (JCPDS 41-1442). For pure Fe_2O_3 catalyst, the typical diffraction peaks of α- Fe_2O_3 (JCPDS 79-7) were identified. For the binary oxide materials, as the addition of iron species increased, the diffraction signals of MnO_2 became increasingly weaker, with $MnFe_{0.75}$ catalyst showing the weakest intensity. This phenomenon could be interpreted by the introduction of Fe ions into the MnO_2 lattice, leading to the generation of a more non-crystalline phase of MnO_2 [8]. This could further enhance the occurrence of the lattice defects and exposure of inner atoms, improve the surface area of materials [9], which could be beneficial to the catalytic activity. The results catalytic activity showed that the catalytic performance firstly increased and then decreased with increasing the molar ratio of Fe/Mn, with with $MnFe_{0.75}$ catalyst exhibiting the highest catalytic performance.

3.2. Design of experimental analysis

3.2.1. Model and adequacy check

The RSM based on the central composite design (CCD) was applied to investigate the relationship between the key process variables such as discharge power (1-5 W), gas flow rate (0.5-1.5 L·min^{-1}) and molar ratio of Fe/Mn (0.25-1.25) in terms of the formaldehyde removal efficiency. The relationships between the input process parameters and the output response were estimated using quadratic models as shown in Eq. (2). The analysis of variance showed that the R^2 of the fitting models are over 0.99, indicating that the selected model provided a good prediction of response variables. This also could be confirmed by the diagnostic plots as shown in Fig. 3.

$$Y_1 = 58.98 + 12.16X_1 - 7.34X_2 - 1.71X_3 - 0.6475X_1X_2 - 0.1625X_1X_3 - 0.2315X_2X_3 + 0.1133X_1^2 - 0.3242X_2^2 - 2.94X_3^2 \quad (2)$$

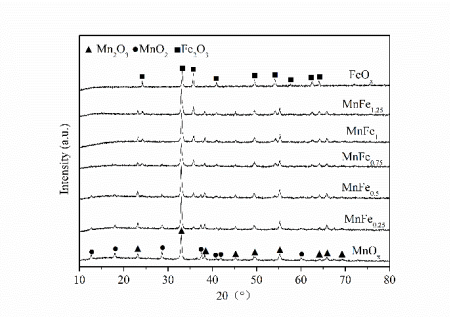

Fig.2 XRD patterns of MnO_x-Fe_2O_3 catalysts

3.2.2. Effect of discharge power and gas flow rate

The two-dimensional (2D) contour and three-dimensional (3D) surface plots of the response functions were used to determine both the main and the interaction effects of the variables such as the discharge power and gas flow rate. The interactive influence among the various variables could be displayed by the 3D surface plot directly and the degree of the interaction effect could be reflected by the shape of the contour lines in the 2D plot. The combined effect of discharge power and gas flow rate on the formaldehyde removal efficiency and with the molar ratio of Fe/Mn setting as 0.75 was shown in Fig. 4. Based on the plane shape of the fitting response surface and the almost straight contour lines, it is concluded that the interaction between the discharge power and gas flow rate was insignificant. It was obvious that compared with the gas flow rate, the discharge power played a major role in affecting the formaldehyde removal efficiency. Thus, high discharge power and low gas flow rate were conducive to achieve better formaldehyde removal efficiency.

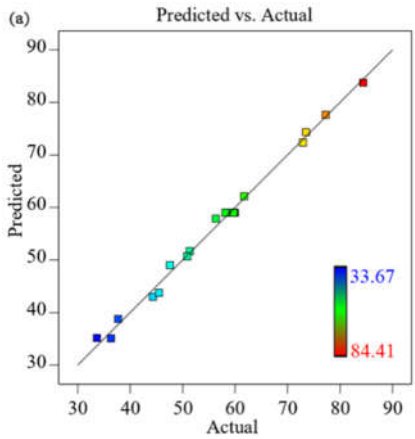

Fig. 3 Comparison of experimental and predicted results of formaldehyde removal efficiency

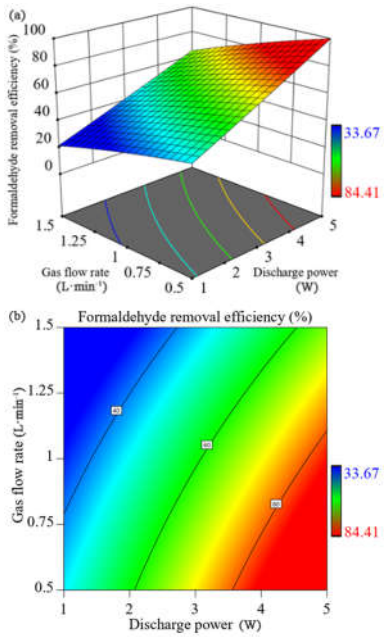

Fig. 4 Effect of discharge power and gas flow rate on the formaldehyde removal efficiency ((a):3D surface plot; (b), projected contour plot)

4. Conclusion

In this study, the formaldehyde removal in the NTP-catalytic system over a series of MnO_x-Fe_2O_3 catalysts was investigated. The effects of various experimental parameters such as discharge power, gas flow rate and molar ratio of Fe/Mn on the formaldehyde removal in the NTP-catalytic reaction process and the interactions between these variables were investigated using a CCD method based on RSM. The results showed that the developed model provided a good prediction of response variables. The gas flow rate has a less significant role than the discharge power for the removal of formaldehyde.

5. Acknowledgements

This research was financially supported by the National Science Foundation of China (41573138), State Key Laboratory of Loess and Quaternary Geology, Institute of Earth Environment, CAS (SKLLQG1616) and China Scholarship Council (No. 201806280087). Yu Huang is also supported by the "Hundred Talent Program" of the Chinese Academy of Sciences.

6. References

[1] W.J. Liang, J. Li, J.X. Li, T. Zhu, Y.Q. Jin, Journal of hazardous materials, **175**, 1090 (2010).
[2] T. Salthammer, S. Mentese, R. Marutzky, Chemical Reviews, **110**, 2536 (2010).
[3] S. Lu, K. Li, F. Huang, C. Chen, B. Sun, Applied Surface Science, **400**, 277 (2017).
[4] R. Fang, H. Huang, J. Ji, M. He, Q. Feng, Y. Zhan, D.Y.C. Leung, Chemical Engineering Journal, **334**, 2050 (2018).
[5] L. Lu, H. Tian, J. He, Q. Yang, The Journal of Physical Chemistry C, **120**, 23660 (2016).
[6] X. Zhu, X. Gao, R. Qin, Y. Zeng, R. Qu, C. Zheng, X. Tu, Applied Catalysis B: Environmental, **170-171**, 293 (2015).
[7] Y. Wan, X. Fan, T. Zhu, Chemical Engineering Journal, **171**, 314 (2011).
[8] S. Zhang, Y. Zhao, J. Yang, J. Zhang, C. Zheng, Chemical Engineering Journal, **348**, 618 (2018).
[9] J. Chen, X. Chen, W. Xu, Z. Xu, J. Chen, H. Jia, J. Chen, toluene, Chemical Engineering Journal, **330**, 281 (2017).